Structure evolution of gold cluster anions between the planar and cage structures by isoelectronic substitution: Au_n^- ($n = 13$–15) and MAu_n^- ($n = 12$–14; M = Ag, Cu)

Rhitankar Pal,[1] Lei-Ming Wang,[2,a)] Wei Huang,[2] Lai-Sheng Wang,[2,b)] and Xiao Cheng Zeng[1,c)]
[1]*Department of Chemistry, University of Nebraska-Lincoln, Lincoln, Nebraska 68588, USA*
[2]*Department of Chemistry, Brown University, Providence, Rhode Island 02912, USA*

(Received 9 November 2010; accepted 13 December 2010; published online 1 February 2011)

The structural and electronic effects of isoelectronic substitution by Ag and Cu atoms on gold cluster anions in the size range between 13 and 15 atoms are studied using a combination of photoelectron spectroscopy and first-principles density functional calculations. The most stable structures of the doped clusters are compared with those of the undoped Au clusters in the same size range. The joint experimental and theoretical study reveals a new C_{3v} symmetric isomer for Au_{13}^-, which is present in the experiment, but has *hitherto* not been recognized. The global minima of Au_{14}^- and Au_{15}^- are resolved on the basis of comparison between experiment and newly computed photoelectron spectra that include spin-orbit effects. The coexistence of two isomers for Au_{15}^- is firmly established with convincing experimental evidence and theoretical calculations. The overall effect of the isoelectronic substitution is minor on the structures relative to those of the undoped clusters, except that the dopant atoms tend to lower the symmetries of the doped clusters. © *2011 American Institute of Physics*. [doi:10.1063/1.3533443]

I. INTRODUCTION

Because of the unique catalytic properties discovered for gold nanoparticles,[1] the study of gold clusters has been a central focus in cluster science during the last few years.[2–8] Numerous experimental[9–25] and theoretical studies[14–45] have been devoted to elucidate the structural and electronic properties of small gold clusters. This knowledge on size-selected gold clusters is essential to understanding the catalytic mechanisms exhibited by gold nanoparticles. A number of modern experimental techniques have been used to study size-selected gold clusters, such as ion mobility,[14,15] photoelectron spectroscopy (PES),[16–18,20,21,23,34–36,39–46] mass spectrometry,[47] infrared multiphoton dissociation spectroscopy,[19,25,48] and trapped ion electron diffraction (TIED).[22,41,49] Density functional theory (DFT),[14–45,49–53] in particular when combined with experimental studies, has emerged as one of the most powerful theoretical tools to study the structures of clusters.

Although impressive progresses have been achieved in understanding the most stable structures of small gold clusters, it is quite difficult to completely resolve all the atomic arrangements of energetically closely isomers even for relatively small systems. For instance, we have recently discovered, in a joint experimental and theoretical effort,[36] a new isomer for a cluster as small as Au_7^-, which was not recognized in numerous prior experimental and theoretical studies. The strong relativistic and spin-orbit (SO) coupling effects in gold make it theoretically very challenging to determine the true global minimum structures of even relatively small gold clusters. Therefore, state-of-the-art experimental data, in conjunction with extensive theoretical studies, are needed in order to obtain unequivocal structural information of gold clusters. Indeed, on the basis of the experimental and theoretical explorations over the last decade, many structural issues of small gold clusters have been resolved. One of the most interesting early finding was the planar (2D) gold cluster anions for Au_n^- ($n < 12$) owing to the strong relativistic effects.[2,3,14] The discoveries of the golden cages[21] from Au_{16}^- to Au_{18}^- and the Au_{20}^- pyramid[17] represent two other milestones in the studies of structural evolution of gold clusters.

Recently, we have found that Ar-tagging and O_2-titration can be used effectively to resolve isomers for gold cluster anions in combination with PES.[34–36] For example, using Ar-tagging we confirmed the coexistence of both the 2D and 3D isomers in the cluster beam of Au_{12}^- and obtained isomer-specific photoelectron spectra for this critical cluster.[35] We have also been able to determine decisively that the Au_{10}^- beam contained unprecedentedly four co-existing isomers.[42] The cage-to-pyramid structural transition at Au_{18}^- has also been resolved recently using Ar-tagging and O_2-titration, in combination with DFT calculations.[34]

We have found that doping by Cu and Ag is also an effective means to resolve isomers in the undoped gold clusters because the isoelectronic substitutions do not change significantly the geometries and electronic structures of the parent gold clusters.[36,42] This is particularly effective when Ar-tagging or O_2-titration is not sufficient to resolve the isomers, such as in Au_7^-.[36] Because the Cu or Ag substitution can slightly alter the relative stability of the closely lying gold cluster isomers, the isoelectronic substitutions can enhance the abundance of a given isomer relative to that of the undoped clusters. Such strategy allowed us to successfully

a)Present address: Department of Physics, University of Pittsburgh, Pittsburgh, Pennsylvania 15260, USA.
b)Electronic mail: lai-sheng_wang@brown.edu.
c)Electronic mail: xczeng@phase2.unl.edu.

identify a new isomer for Au_7^-, a Au atom attached to the corner of a triangular Au_6, which was always present in the experiment, but was not recognized.[36] The Cu or Ag substitution slightly favors the 3D structures near the size range of 2D-to-3D structural transition, decreased the critical size of the 2D-to-3D transition in Au_{12}^- to the eleven-atom clusters, MAu_{10}^-, while breaking the near degeneracy of the 2D and 3D isomers in Au_{12}^-, allowing only the 3D MAu_{11}^- clusters to be observed experimentally.[42] Here we continue our investigation of the effect of isoelectronic substitution on the post-2D clusters Au_{13}^- – Au_{15}^- by Ag and Cu atoms. It should be pointed out that the precise structures and isomers of the anionic gold clusters in this size range are still not well understood.[16,21,22,29] Using the isoelectronic substitutions and DFT calculations with the inclusion of the SO effects, we have identified new isomers and fully resolved all isomers and structures for clusters in the size range between the 2D and cage structures.

II. EXPERIMENTAL METHODS

The experiments were performed on a magnetic-bottle PES apparatus equipped with a laser vaporization supersonic cluster source, details of which have been published elsewhere.[44] The $AgAu_n^-$ and $CuAu_n^-$ clusters were produced by laser vaporization of a Au/Ag and Au/Cu mixed disk target containing about 7% Ag and Cu, respectively. A time-of-flight mass spectrometer was used to analyze the negatively charged clusters extracted perpendicularly from the cluster beam. Clusters of interest were selected and decelerated before being intercepted by a 193 nm laser beam from an ArF excimer laser for photodetachment. The amount of dopant in the target was carefully tuned to low concentrations such that the chances of multiple doping were minimized and the MAu_n^- series with a single dopant atom were optimized in order to achieve clean mass selections. Photoelectrons were collected and measured by the magnetic-bottle time-of-flight electron energy analyzer and calibrated by the known spectrum of Au^-. The resolution of the apparatus was $\Delta E/E \sim 2.5\%$, i.e., about 25 meV for 1 eV electrons.

III. THEORETICAL METHODS

The basin-hopping (BH) global minimum search[54] coupled with a DFT optimization method was employed to search for the lowest-lying isomers of doped MAu_n^- (n = 12–14 and M = Ag, Cu) clusters. The computer code, originally developed for studying silicon clusters,[55] was extended to treat doped clusters. Generalized gradient approximation with the Perdew–Burke–Ernzerhof (PBE) functional was chosen for the DFT optimization.[56,57] Multiple randomly constructed isomer structures were used as initial inputs for the BH search program. The BH program generated a few hundreds isomers for MAu_{13}^- and MAu_{14}^- to a thousand isomers for MAu_{12}^-. For the latter, however, many isomers were 2D. In a previous paper,[42] we showed that the 2D-to-3D transition occurred at MAu_{11}^-. Hence, we only collected 3D low-lying isomers of MAu_{12}^- for computing their photoelectron spectra. For MAu_{13}^- and MAu_{14}^-, we collected those low-lying isomers within 0.2 eV from the lowest-lying isomer for computing their photoelectron spectra and comparing with the experimental spectra.

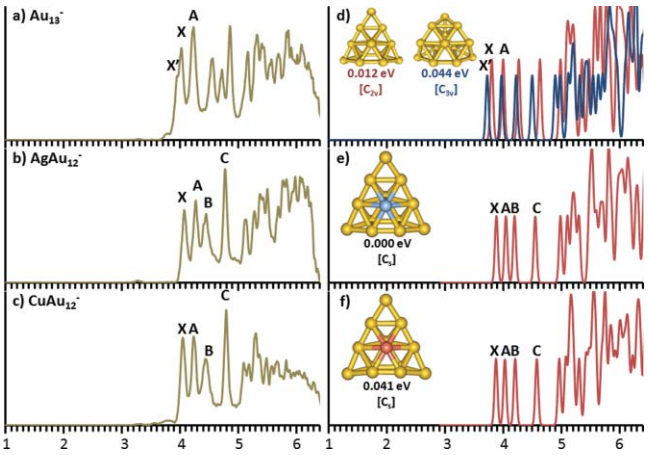

FIG. 1. Photoelectron spectra of Au_{13}^-, $AgAu_{12}^-$, and $CuAu_{12}^-$ at 193 nm (6.424 eV) (left) compared with computed spectra and the cluster structures (right). Au—golden, Ag—blue, and Cu – red.

Our recent joint experimental and theoretical studies of gold clusters indicate the necessity of inclusion of the SO effects to achieve quantitative agreement between the experimental and theoretical photoelectron spectra.[34,36,42,43] We also used the PBE0 hybrid functional[57] and the CRENBL basis set as implemented in the NWCHEM 5.1.1 software package[58] for optimization of all the aforementioned low-lying anionic clusters. We then performed single-point energy calculations at the SO-PBE0/CRENBL level of theory implemented in NWCHEM 5.1.1. Finally, the energies of the neutral isomers of each species were computed at the SO-PBE0/CRENBL level of theory but in the corresponding anion geometry. The first vertical detachment energies (VDEs) of the anionic clusters were calculated as the difference between the energies of the neutral and anionic species of each isomer. The binding energies of the deeper occupied orbitals of the anion (i.e., the density of states) were then added to the first VDE to approximate higher binding energy features. Each computed VDE was fitted with a Gaussian width of 0.035 eV to yield the computed spectrum which was compared with the experimentally observed spectrum. For several species (e.g., Au_{13}^-, Au_{15}^-, M Au_{14}^-, etc.) the computed spectra of at least two isomers had to be combined in order to accurately reproduce their corresponding experimental spectrum. In these cases, the spectral intensities of the minor isomer were uniformly scaled by a factor such that the scaling factor was guided by the ratio of the measured intensity of the first peak of the major isomer to that of the minor isomer.

IV. EXPERIMENTAL RESULTS

The experimental photoelectron spectra of Au_{n+1}^- and MAu_n^- (n = 12–14; M = Ag, Cu) are presented in Figs. 1–3, respectively (the left panels). The spectra for the three undoped gold clusters (Au_{13}^-, Au_{14}^-, and Au_{15}^-) have been presented before.[12,16] They are shown here for comparison with those of the doped clusters. However, as will be seen

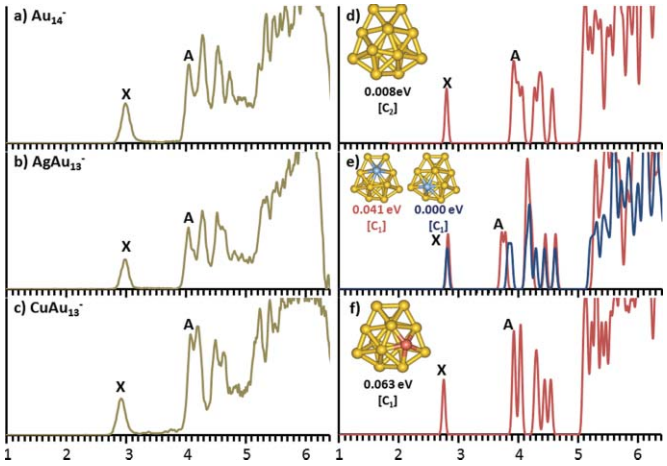

FIG. 2. Photoelectron spectra of Au_{14}^-, $AgAu_{13}^-$, and $CuAu_{13}^-$ at 193 nm (left) compared with computed spectra and the cluster structures (right). Au—golden, Ag—blue, and Cu—red.

below, the spectrum of Au_{13}^- consists of contributions from at least two isomers, whereas for Au_{15}^- the structures found in the current study are different from the previous study. The computed spectra of the low-lying isomers which yield the best agreement with the experimental spectra are also presented (the right panels) for comparison (*vide infra*). Both experimental and theoretical first VDEs of the undoped and doped clusters are given in Table I.

A. Au_{13}^- and MAu_{12}^-

The photoelectron spectrum of Au_{13}^- [Fig. 1(a)] shows five well resolved PES bands in the low binding energy region below 5 eV. The five peaks are closely spaced followed by a small gap and the congested region (due to gold 5d orbitals) at higher binding energies. Careful examination shows that there is a shoulder (X′) on the lower binding energy side of band X, suggesting the presence of a possible minor isomer. At 266 nm, the shoulder was better resolved, but the previous joint PES and DFT study did not consider the structures of Au_{13}^-.[16] Interestingly, the photoelectron spectra of $AgAu_{12}^-$ and $CuAu_{12}^-$ [Figs. 1(b) and 1(c)] appear similar to each other, suggesting that these two clusters should have similar structures. The spectra of the doped clusters are simpler in comparison to that of Au_{13}^- [Fig. 1(a)], consistent with the suggestion of multiple isomers in the spectra of the undopted cluster. The spectra of the doped clusters [Figs. 1(b) and 1(c)] consist of three almost evenly spaced peaks (X, A, and B) and another sharp and intense band C (~4.8 eV) below 5 eV. A careful examination reveals that the spectrum of Au_{13}^- also displays a similar sharp and intense peak at ~4.8 eV, suggesting that one of the isomers of Au_{13}^- in the cluster beam may have the structure similar to that of MAu_{12}^-.

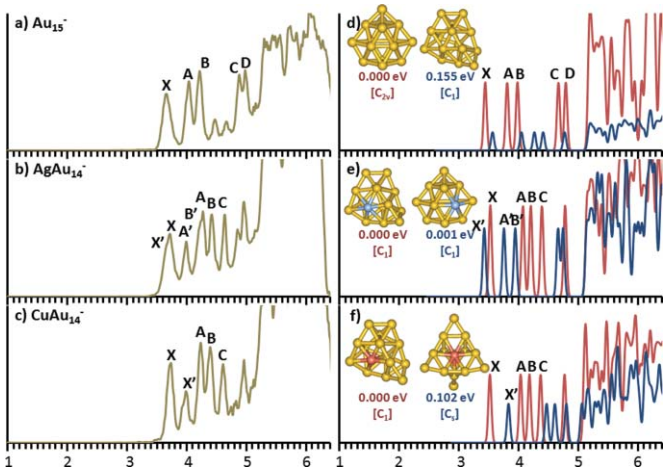

FIG. 3. Photoelectron spectra of Au_{15}^-, $AgAu_{14}^-$, and $CuAu_{14}^-$ at 193 nm (left) compared with computed spectra and the cluster structures (right). Au—golden, Ag—blue, and Cu—red.

TABLE I. Experimental and calculated (at PBE0/CRENBL level) values [in electron volts (eV) units] of the first VDEs of the major isomers of MAu_n^- and Au_{n+1}^-. The values in parenthesis refer to the uncertainty in the last digits of the experimental data.

n	Isomers	VDE (expt.) (eV)	VDE (theory) (eV)
12	Au_{13}^-	4.02 (3)	3.79[a]
			3.71[b]
	$AgAu_{12}^-$	4.07 (3)	3.87[a]
	$CuAu_{12}^-$	4.04 (3)	3.87[a]
13	Au_{14}^-	2.95 (3)	2.80[a]
	$AgAu_{13}^-$	2.95 (3)	2.80[a]
			2.79[b]
	$CuAu_{13}^-$	2.88 (3)	2.81[a]
14	Au_{15}^-	3.63 (3)	3.43[a]
			3.54[b]
	$AgAu_{14}^-$	3.69 (3)	3.51[a]
			3.41[b]
	$CuAu_{14}^-$	3.70 (3)	3.50[a]
			3.81[b]

[a]VDE of major isomer.
[b]VDE of minor isomer.

B. Au_{14}^- and MAu_{13}^-

The three 14-atom clusters (Au_{14}^-, $AgAu_{13}^-$, and $CuAu_{13}^-$) display relatively simple and similar PES patterns [Figs. 2(a)–2(c)], implying that only one major isomer exists in the cluster beam and they all have similar structures. The neutral 14-atom clusters, Au_{14} and MAu_{13}, are closed-shell with large HOMO–LUMO gaps, resulting in significantly lower first VDEs relative to those of the 13-atom clusters (Table I). The X band corresponds to removal of the extra electron entering the LUMO of the neutral clusters. Detachment from orbitals corresponding to the neutral HOMO or deeper orbitals results in both triplet and singlet final states, which could not be resolved and led to spectral broadening for all the 14-atom clusters in comparison to those of the 13-atom clusters. Indeed, the A band of Au_{14}^- was resolved into two components due to the triplet and singlet splitting at 266 nm, as reported previously.[16]

C. Au_{15}^- and MAu_{14}^-

The spectrum of Au_{15}^- displays five intense peaks (X, A–D) and two weak peaks between bands B and C in the

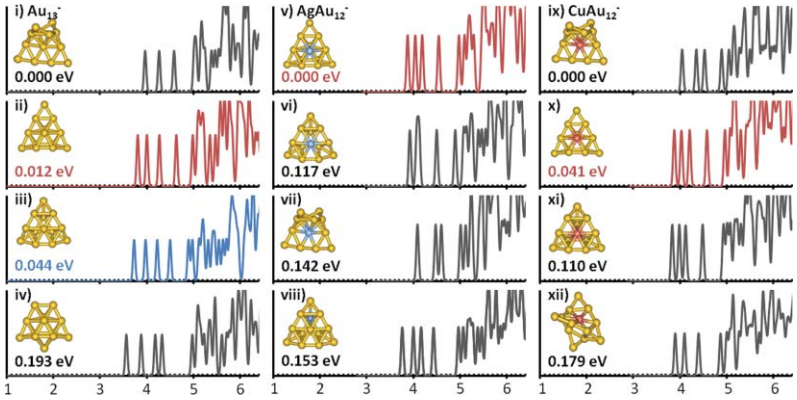

FIG. 4. The four lowest-lying structures for Au_{13}^- (i)–(iv) and MAu_{12}^- [Ag: (v)–(viii); Cu: (ix)–(xii)] ranked according to their relative energies and the computed spectra calculated at the SO-PBE0/CRENBL level of theory. Spectra presented in Fig. 1 are highlighted in red and blue.

low binding energy region below 5.0 eV [Fig. 3(a)]. Since Au_{15}^- is closed shell, each occupied orbital should result in one PES band and all the bands should have similar intensities. Therefore, the two weak features provide evidence for the presence of a minor isomer in the Au_{15}^- beam.[21] The spectra of the two doped clusters MAu_{14}^- [Figs. 3(b) and 3(c)] appear more complicated than those of the undoped clusters, suggesting that they may contain contributions from different isomers. The broad spectral widths of the X and A bands in $AgAu_{14}^-$ [Fig. 3(b)] and the weak band (X′) in the spectrum of $CuAu_{14}^-$ are all consistent with the presence of minor isomers. As will be shown below, these experimental observations are borne out from the theoretical calculations.

V. THEORETICAL RESULTS AND DISCUSSIONS

The structures of the three clusters (Au_{13}^-, Au_{14}^-, and Au_{15}^-) have been extensively studied previously.[2,3,7,8,16,21,22,24,49,50] In the current study, we focus on our effort on the doped clusters. We are interested in how the isoelectronic doping affects the overall energetics and structures of the different isomers found for the undoped clusters. The comparisons between the computed spectra and the experimental spectra are critical to gain confidence about the computed low-lying structures. As we have shown before, the inclusion of the SO effect was essential in the computed spectra and allowed us to achieve almost quantitative comparison between the experiment and theory. The computed spectra from low-lying isomers that agree best with the experimental data are shown in Figs. 1–3 . All the low-lying isomers considered and their computed spectra are shown in Figs. 4–6 for Au_{n+1}^- and MAu_n^- (n = 12–14, M = Ag and Cu), respectively. Cartesian coordinates of all isomers are given in the supplementary materials.[59]

A. Au_{13}^- and MAu_{12}^-

As reported previously, theoretical VDEs are slightly lower than the experimental VDEs by 0.1–0.3 eV due to the inclusion of SO effects in the calculations.[36,42,43] The computed spectra [Fig. 1(d)] generated from the two best candidate structures chosen for Au_{13}^- well reproduce the experimental spectrum: the C_{2v} isomer is the dominant one corresponding to stronger PES bands and the C_{3v} structure

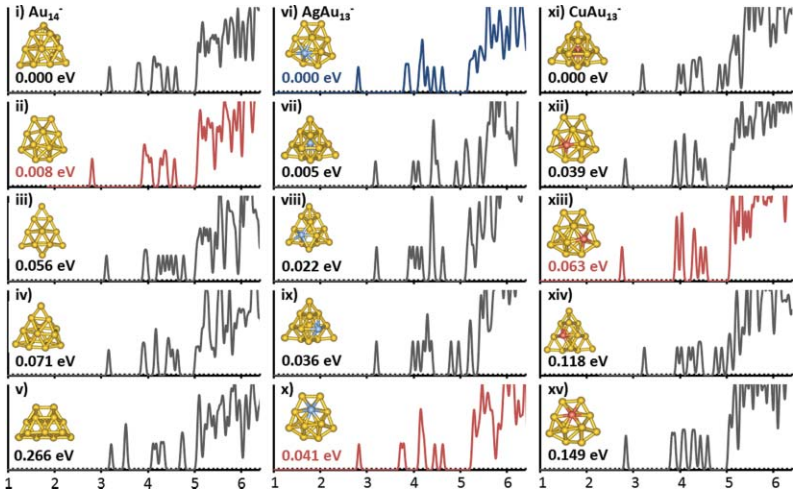

FIG. 5. The five lowest-lying structures for Au_{14}^- (i)–(v) and MAu_{13}^- [Ag: (vi)–(x); Cu: (xi)–(xv)] ranked according to their relative energies and the computed spectra calculated at the SO-PBE0/CRENBL level. Spectra presented in Fig. 1 are highlighted in red and blue.

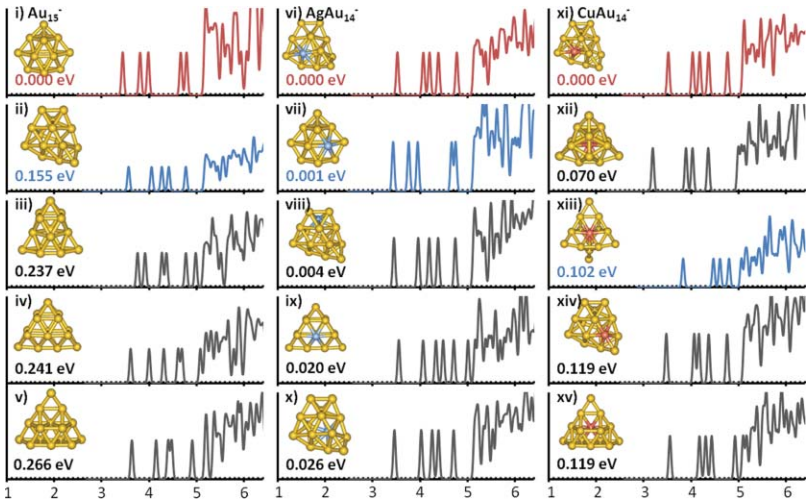

FIG. 6. The five lowest-lying structures for Au_{15}^- (i)–(v) and MAu_{14}^- [Ag: (vi)–(x); Cu: (xi)–(xv)] ranked according to their relative energies and the computed spectra calculated at the SO-PBE0/CRENBL level. Spectra presented in Fig. 1 are highlighted in red and blue.

can be considered as the minor isomer corresponding to weaker PES bands. As can be seen from Fig. 1, although the lowest-energy Au_{13}^- isomer is **i**, the C_{2v} (isomer **ii**) and C_{3v} (isomer **iii**) structures together give rise to excellent agreement with the experimental spectrum. Both these isomers (**ii** and **iii**) are energetically very close to the lowest lying isomer **i** with only 0.012 and 0.044 eV higher in energy, respectively. We have shown before that such small differences in energy are likely due to the intrinsic errors of DFT calculations and the spectral pattern is much more reliable in structure assignments than the small difference in relative energies.[36,42,43] Structure **i** (Fig. 4) can be ruled out because its computed spectrum does not agree well with the experimental spectrum. The major isomer of Au_{13}^- [Fig. 1(d), highlighted in red] has been reported before,[16,22] it possesses a C_{2v} structure and can be made by adding a Au atom to the 3D isomer of Au_{12}^-. The C_{3v} isomer [Fig. 1(d) shown in blue color] has also been reported previously,[24,49] which can be viewed as generated from the C_{2v} isomer by slightly displacing the central gold atom from one of the faces. The C_{2v} isomer can be viewed as a two-layer structure: a gold triangle stacking on top of the Au_{10}^- triangle [Fig. 1(d)].

Because of the similarity of their photoelectron spectra [Figs. 1(b) and 1(c)], the structures of the $AgAu_{12}^-$ and $CuAu_{12}^-$ clusters are expected to be similar. Structures **v** and **x** (Fig. 4) gave the best agreement with the experimental spectra for $AgAu_{12}^-$ and $CuAu_{12}^-$, respectively. Indeed, the structures of $AgAu_{12}$- and $CuAu_{12}^-$ are nearly identical to the C_{2v} isomer of Au_{13}^- by substituting a Au atom. The substitution site is consistent with our recent studies,[36,42] which show that Ag or Cu atom tends to locate in the center of a gold planar hexagon in doped Au_n^- clusters. It should be noted here that although the lowest-energy isomer **v** of $AgAu_{12}^-$ gives the best agreement to the experimental spectrum, the second lowest-energy isomer **x** (0.041 eV higher in energy than **ix**) of $CuAu_{12}^-$ is found to be the predominant species. Both the lowest-lying isomer **ix** and **x** of $CuAu_{12}^-$ were reported previously[50] but now as a result of the inclusion of SO effects, their energy difference is further reduced, which lends more credence toward the assignment.

B. Au_{14}^- and MAu_{13}^-

The Au_{14}^- cluster has been studied by a number of groups using different experimental and computational methods.[16,22,29,33,49] Our BH searches consistently yield the same low-lying isomers, and the five lowest-lying isomers with their relative energies and computed spectra are given in Fig. 5(**i**–**v**). Because these isomers are very close in energy, it is difficult to identify the true global minima due to the intrinsic errors in DFT calculations. Based on previous calculations on gold clusters at the SO-PBE0/CRENBL level,[58] the calculated first VDEs are usually underestimated relative to the experimental values by 0.1–0.3 eV. Among the four lowest-lying isomers, only the first VDE of structure **ii** (2.80 eV) is slightly lower than the experimental VDE (2.95 eV) (see Table I), while the other three isomers (**i**, **iii**, and **iv**) give relatively high first VDEs (>3 eV). Isomer **ii** is only 0.008 eV higher in energy than the lowest-lying isomer (**i**) and it is well within the DFT error to compete for the global minimum. Our experimental data [Fig. 2(a)] suggest that Au_{14}^- consisted of a single isomer. By comparing the computed spectra with the experimental data, we find that isomer **ii** gives the best agreement in terms of the spectral features below 5.0 eV [Fig. 2(d)]. Isomer **ii** has C_2 symmetry and it is similar to the structure reported by Schooss and co-workers using trapped ion electron diffraction combined with DFT calculations.[49] Note again that Au_{14}^- is an open-shell cluster and the photoelectron spectrum contains transitions to both singlet and triplet final states, which cannot be well reproduced using the current theoretical calculations. This may explain partly the differences between the computed spectrum and the experimental data. In our previous studies,[42] we have showed that for open-shell clusters such as Au_{12}^- the computed spectra using our method can reproduce the overall pattern of the

experimental photoelectron spectra, but may not yield quantitative agreement with the experiment such as closed shell anionic cluster.

The Ag and Cu doped clusters show similar photoelectron spectra [Figs. 2(b)–2(c)] to that of Au_{14}^- and are therefore expected to possess similar structures. Our BH searches generated many low-lying structures and the five lowest-lying isomers are presented in Figs. 5(**vi**)–5(**xv**). Similar to Au_{14}^- the isomers for MAu_{13}^- also have very close energies and the global minima can only be identified by comparing the computed spectra with experiment data. Taking into account that the VDEs are slightly underestimated by the SO-PBE0 method, we can exclude three of the $AgAu_{13}^-$ isomers **vii–ix** (Fig. 5), because their VDEs are higher than the experimental value of 2.95 eV (Fig. 2; Table I). Isomers **vi** and **x** produce very similar PES patterns in the computed spectra [Figs. 5(**vi**) and 5(**x**)] and are also energetically very close (within 0.04 eV). Note that each surface of the parent Au_{14}^- C_2 structure has three distinct sites—two hexagonal sites and one with a pentagonal motif. Isomers **vi** and **x** are derived from the Au_{14}^- structure where one gold atom in the two hexagonal sites is replaced by a Ag atom. It is difficult to finalize the assignment based only on the minor difference of these two isomers. However, when examining carefully at the experimental spectrum of $AgAu_{13}^-$ [Fig. 2(b)], one can find that there is a weak feature located on the right shoulder of the A band, which is well reproduced by isomer **vi** [Fig. 2(e)]. Thus, it is likely that isomers **vi** and **x** were both present in the cluster beam.

For $CuAu_{13}^-$, isomer **xi** and **xiv** can be ruled out due to their higher calculated binding energies (Fig. 5). The other three isomers [Figs. 4(**xii**)–4(**xiii**) and 4(**xv**)] are formed by replacing one Au atom from the surface of the parent Au_{14}^-. The computed spectrum of isomer **xv** is quite different from the experimental spectrum and can be ruled out. Similar to $AgAu_{13}^-$, it is difficult to assign global minimum between isomers **xii** and **xiii**, because they have very similar structures, similar computed spectral patterns, and very close energies. We tentatively assign isomer **xiii** because its computed spectrum is in slightly better agreement with the experiment, in particular, the splitting between the second and third peaks [Fig. 2(f)].

C. Au_{15}^- and MAu_{14}^-

The computed spectra for the five lowest-lying isomers of Au_{15}^- and MAu_{14}^- are shown in Fig. 6. The computed spectrum of the lowest-energy isomer **i** is in quantitative agreement with the more intense bands in the experimental data [Fig. 3(d)] and can be concluded unequivocally to be the global minimum of Au_{15}^-. The weak features in the experimental data between 4.4–4.8 eV are reproduced very well by the computed spectrum of isomer **ii**, confirming the coexistence of two isomers for Au_{15}^- in the cluster beam.[21] The global minimum of Au_{15}^- possesses C_{2v} symmetry while the minor isomer has a C_1 structure. The energies of these two isomers are close but are much lower than the other low-lying isomers (Fig. 6). Note that both the C_{2v} and C_1 isomers have been reported previously.[21,49] In our previous calculations of the photoelectron spectra for the C_{2v} and C_1 isomers (Au_{15d}^- and Au_{15a}^- in Ref. 21), the SO effects were not included. Because the computed spectra without including the SO effects were only in qualitative but not quantitative agreement with the experimental data, we could not determine unequivocally which isomer between the two was the true global minimum, although the C_1 isomer was tentatively assigned as the major isomer (Au_{15a}^-) in Ref. 21.

The two lowest-energy structures of $AgAu_{14}^-$ are based on the C_{2v} and C_1 isomers of the parent Au_{15}^- and they are nearly degenerate within 0.001 eV (Fig. 6). The computed spectra of these two isomers of $AgAu_{14}^-$ are in excellent agreement with the experimental spectrum [Figs. 3(b) and 3(e)]. In the experimental spectrum, the intensities of the two isomers are similar, consistent with the nearly degeneracy of the two isomers. The isomer based on the C_1 parent of Au_{15}^- has slightly higher intensity and slightly lower in energy and is likely the global minimum for $AgAu_{14}^-$. It should be pointed out that the computed spectra of the two doped clusters are nearly identical to those of their corresponding isomers of the parent Au_{15}^- [Figs. 3(d) and 3(e)]. This observation suggests that the Ag doping induces very little structural change and provides further credence to the assignments for the structures of $AgAu_{14}^-$.

The computed spectra of five lowest-lying isomers for $CuAu_{14}^-$ are shown in Figs. 6(**xi**)–6(**xv**). The lowest-energy structure [Fig. 6(**xi**)] yields a computed spectrum in excellent agreement with the experimental spectrum [Figs. 3(c) and 3(f)], confirming the global minimum for $CuAu_{14}^-$. This structure is identical to the global minimum for $AgAu_{14}^-$ and their computed spectra are also very similar. However, the minor isomer for $CuAu_{14}^-$ is very different from that for $AgAu_{14}^-$, as can be seen from the slightly different experimental spectral patterns [Figs. 3(b) and 3(c)]. Among the four lowest-lying isomers, the computed spectrum of isomer **xiii** (Fig. 6) gives the best agreement with the weak feature X′ [Figs. 3(c) and 3(f)]. The global minimum of $CuAu_{14}^-$ is formed by replacing a Au atom from the C_1 isomer of the parent Au_{15}^-. The minor isomer of $CuAu_{14}^-$ on the other hand is very different from the minor isomer of $AgAu_{14}^-$: it has C_s symmetry with a dangling Au atom. It should be pointed out that we have previously observed dangling gold atoms in observed isomers for Au_7^-, $AgAu_6^-$, and $CuAu_6^-$, all having a very stable triangular Au_6 or MAu_5 core with one Au atom attaching to one corner site.[36] An isomer with a dangling Au atom was also observed for $SiAu_{16}^-$.[51]

VI. CONCLUSION

We present a joint experimental and theoretical study of the structural and electronic effects of isoelectronic substitution by Ag and Cu atoms on anionic gold clusters in the size range of 13–15 atoms. The excellent agreement between the experimental PES data and computed spectra with the inclusion of the spin-orbit effects has allowed us to fully resolve the global minimum structures and low-lying isomers for the clusters, Au_{13}^- to Au_{15}^-. For Au_{13}^-, we found a new C_{3v} isomer, which is nearly degenerate with the global minimum

C_{2v} structure and is present experimentally, but not recognized previously. The doped clusters with Ag or Cu atoms are shown to derive from the parent clusters with minimal structural changes. A minor isomer of $CuAu_{14}^-$ was an exception, whose structure features a dangling Au atom and is not related to the structures of Au_{15}^-. This study reinforces the importance of including the spin-orbit effects in calculating the density of states of gold clusters and using isoelectronic substitution in resolving structures and low-lying isomers for gold clusters.

ACKNOWLEDGMENTS

The experimental work was supported by the National Science Foundation (CHE-1036387 to L.S.W.). The theoretical work done using NWCHEM was performed on supercomputers at the PNNL EMSL Molecular Science Computing Facility and in the University of Nebraska's Holland Computing Center. The theoretical work done at UNL was supported by grant from the National Science Foundation (Grant Nos. DMR-0820521 and EPS-1010094), ARO (Grant No. W911NF1020099), and the Nebraska Research Initiative, and a seed grant from Nebraska Public Power District through the Nebraska Center for Energy Sciences Research.

[1] M. Haruta, Catal. Today **36**, 153 (1997).
[2] P. Pyykkö, Angew. Chem., Int. Ed. **43**, 4412 (2004).
[3] P. Pyykkö, Inorg. Chim. Acta **358**, 4113 (2005).
[4] P. Koskinen, H. Häkkinen, B. Huber, B. v. Issendorff, and M. Moseler, Phys. Rev. Lett. **98**, 051701 (2007).
[5] R. M. Olson and M. S. Gordon, J. Chem. Phys. **126**, 214310 (2007).
[6] P. Pyykkö, Nat. Nanotechnol. **2**, 273 (2007).
[7] H. Häkkinen, Chem. Soc. Rev. **37**, 1847 (2008).
[8] P. Pyykkö, Chem. Soc. Rev. **37**, 1967 (2008).
[9] J. Ho, K. M. Ervin, and W. C. Lineberger, J. Chem. Phys. **93**, 6987 (1990).
[10] G. A. Bishea and M. D. Morse, J. Chem. Phys. **95**, 8779 (1991).
[11] G. F. Gantefor, D. M. Cox, and A. Kaldor, J. Chem. Phys. **96**, 4102 (1992).
[12] K. J. Taylor, C. L. Pettiettehall, O. Cheshnovsky, and R. E. Smalley, J. Chem. Phys. **96**, 3319 (1992).
[13] B. A. Collings, K. Athanassenas, D. Lacombe, D. M. Rayner, and P. A. Hackett, J. Chem. Phys. **101**, 3506 (1994).
[14] F. Furche, R. Ahlrichs, P. Weis, C. Jacob, S. Gilb, T. Bierweiler, and M. M. Kappes, J. Chem. Phys. **117**, 6982 (2002).
[15] S. Gilb, P. Weis, F. Furche, R. Ahlrichs, and M. M. Kappes, J. Chem. Phys. **116**, 4094 (2002).
[16] H. Häkkinen, B. Yoon, U. Landman, X. Li, H. J. Zhai, and L. S. Wang, J. Phys. Chem. A **107**, 6168 (2003).
[17] J. Li, X. Li, H. J. Zhai, and L. S. Wang, Science **299**, 864 (2003).
[18] H. Häkkinen, M. Moseler, O. Kostko, N. Morgner, M. A. Hoffmann, and B. von Issendorff, Phys. Rev. Lett. **93**, 093401 (2004).
[19] A. Fielicke, A. Kirilyuk, C. Ratsch, J. Behler, M. Scheffler, G. von Helden, and G. Meijer, Phys. Rev. Lett. **93**, 023401 (2004).
[20] M. Ji, X. Gu, X. Li, X. G. Gong, J. Li, and L. S. Wang, Angew. Chem., Int. Ed. **44**, 7119 (2005).
[21] S. Bulusu, X. Li, L. S. Wang, and X. C. Zeng, Proc. Natl. Acad. Sci. U.S.A. **103**, 8326 (2006).
[22] X. Xing, B. Yoon, U. Landman, and J. H. Parks, Phys. Rev. B **74**, 165423 (2006); B. Yoon, P. Koskinen, B. Huber, O. Kostko, B. von Issendorff, H. Häkkinen, M. Moseler, and U. Landman, ChemPhysChem **8**, 157 (2007).
[23] X. Gu, S. Bulusu, X. Li, X. C. Zeng, J. Li, X. G. Gong, and L. S. Wang, J. Phys. Chem. C **111**, 8228 (2007).
[24] M. P. Johansson, A. Lechtken, D. Schooss, M. M. Kappes, and F. Furche, Phys. Rev. A **77**, 053202 (2008).
[25] P. Gruene, D. M. Rayner, B. Redlich, A. F. G. Van Der Meer, J. T. Lyon, G. Meijer, and A. Fielicke, Science **321**, 674 (2008).
[26] H. Häkkinen and U. Landman, Phys. Rev. B **62**, R2287 (2000).
[27] R. Wesendrup, T. Hunt, and P. Schwerdtfeger, J. Chem. Phys. **112**, 9356 (2000).
[28] H. Häkkinen, M. Moseler, and U. Landman, Phys. Rev. Lett. **89**, 033401 (2002).
[29] J. Wang, G. Wang, and J. Zhao, Phys. Rev. B **66**, 035418 (2002).
[30] M. P. Johansson, D. Sundholm, and J. Vaara, Angew. Chem., Int. Ed. **43**, 2678 (2004).
[31] A. V. Walker, J. Chem. Phys. **122**, 094310 (2005).
[32] S. Bulusu and X. C. Zeng, J. Chem. Phys. **125**, 154303 (2006).
[33] L. Xiao, B. Tollberg, X. Hu, and L. Wang, J. Chem. Phys. **124**, 114309 (2006).
[34] W. Huang, S. Bulusu, R. Pal, X. C. Zeng, and L. S. Wang, ACS Nano **3**, 1225 (2009).
[35] W. Huang and L. S. Wang, Phys. Rev. Lett. **102**, 153401 (2009).
[36] W. Huang, R. Pal, L. M. Wang, X. C. Zeng, and L. S. Wang, J. Chem. Phys. **132**, 054305 (2010).
[37] Y. Gao, S. Bulusu, and X. C. Zeng, J. Am. Chem. Soc. **127**, 15680 (2005).
[38] Y. Gao, S. Bulusu, and X. C. Zeng, ChemPhysChem **7**, 2275 (2006).
[39] L. M. Wang, S. Bulusu, H.-J. Zhai, X. C. Zeng, and L. S. Wang, Angew. Chem., Int. Ed. **46**, 2915 (2007).
[40] L. M. Wang, R. Pal, W. Huang, X. C. Zeng, and L. S. Wang, J. Chem. Phys. **130**, 051101 (2009).
[41] L. M. Wang, J. Bai, A. Lechtken, W. Huang, D. Schooss, M. M. Kappes, X. C. Zeng, and L. S. Wang, Phys. Rev. B **79**, 033413 (2009).
[42] L. M. Wang, R. Pal, W. Huang, X. C. Zeng, and L. S. Wang, J. Chem. Phys. **132**, 114306 (2010).
[43] N. Shao, W. Huang, Y. Gao, L. M. Wang, X. Li, L. S. Wang, and X. C. Zeng, J. Am. Chem. Soc. **132**, 6596 (2010).
[44] L. S. Wang, H. S. Cheng, and J. W. Fan, J. Chem. Phys. **102**, 9480 (1995).
[45] Y. Negishi, Y. Nakamura, A. Nakajima, and K. Kaya, J. Chem. Phys. **115**, 3657 (2001).
[46] K. Koyasu, Y. Naono, M. Akutsu, M. Mitsui, and A. Nakajima, Chem. Phys. Lett. **422**, 62 (2006).
[47] S. Neukermans, E. Janssens, H. Tanaka, R. E. Silverans, and P. Lievens, Phys. Rev. Lett. **90**, 033401 (2003).
[48] L. Lin, P. Claes, P. Gruene, G. Meijer, A. Fielicke, M. T. Nguyen, and P. Lievens, ChemPhysChem **11**, 1932 (2010).
[49] A. Lechtken, C. Neiss, M. M. Kappes, and D. Schooss, Phys. Chem. Chem. Phys. **11**, 4344 (2009).
[50] S. Zorriasatein, K. Joshi, and D. G. Kanhere, J. Chem. Phys. **128**, 184314 (2008).
[51] L. M. Wang, S. Bulusu, W. Huang, R. Pal, L. S. Wang, and X. C. Zeng, J. Am. Chem. Soc. **129**, 15136 (2007).
[52] W. Bouwen, F. Vanhoutte, F. Despa, S. Bouckaert, S. Neukermans, L. T. Kuhn, H. Weidele, P. Lievens, and R. E. Silverans, Chem. Phys. Lett. **314**, 227 (1999).
[53] H. Tanaka, S. Neukermans, E. Janssens, R. E. Silverans, and P. Lievens, J. Chem. Phys. **119**, 7115 (2003).
[54] D. J. Wales and H. A. Scheraga, Science **285**, 1368 (1999); J. P. K. Doye and D. J. Wales, New J. Chem. **22**, 733 (1998).
[55] S. Yoo and X. C. Zeng, Angew. Chem., Int. Ed. **44**, 1491 (2005); S. Yoo and X. C. Zeng, J. Chem. Phys. **119**, 1442 (2003).
[56] J. P. Perdew, K. Burke, and M. Ernzerhof, Phys. Rev. Lett. **77**, 3865 (1996).
[57] C. Adamo and V. Barone, J. Chem. Phys. **110**, 6158 (1999).
[58] E. J. Bylaska, W. A. d. Jong, N. Govind, K. Kowalski, T. P. Straatsma, M. Valiev, D. Wang, E. Apra, T. L. Windus, J. Hammond, P. Nichols, S. Hirata, M. T. Hackler, Y. Zhao, P.-D. Fan, R. J. Harrison, M. Dupuis, D. M. A. Smith, J. Nieplocha, V. Tipparaju, M. Krishnan, Q. Wu, T. Van Voorhis, A. A. Auer, M. Nooijen, E. Brown, G. Cisneros, G. I. Fann, H. Fruchtl, J. Garza, K. Hirao, R. Kendall, J. A. Nichols, K. Tsemekhman, K. Wolinski, J. Anchell, D. Bernholdt, P. Borowski, T. Clark, D. Clerc, H. Dachsel, M. Deegan, K. Dyall, D. Elwood, E. Glendening, M. Gutowski, A. Hess, J. Jaffe, B. Johnson, J. Ju, R. Kobayashi, R. Kutteh, Z. Lin, R. Littlefield, X. Long, B. Meng, T. Nakajima, S. Niu, L. Pollack, M. Rosing, G. Sandrone, M. Stave, H. Taylor, G. Thomas, J. van Lenthe, A. Wong, and Z. Zhang, NWCHEM 5.1.1, Pacific Northwest National Laboratory, Richland, Washington, 2009.
[59] See supplementary material at http://dx.doi.org/10.1063/1.3533443 for more information on Cartesian coordinates of low-lying isomers shown in Figs. 4–6.